Optimal Design of Solenoid Actuators Driving Butterfly Valves

Peiman N. Mousavi
Assistant Professor
Department of Mechanical and Applied Engineering,
Indiana State University,
Terre Haute, IN 47809
e-mail: peiman.naseradinmousavi@villanova.edu

C. Nataraj
Mr. & Mrs. Robert F. Mortiz,
Sr. Endowed Chair Professor in Engineered Systems,
Department of Mechanical Engineering,
Villanova University,
Villanova, PA 19085
e-mail: nataraj@villanova.edu

Smart valves are used in cooling applications and are responsible for regulating and supplying the coolant, which is critical for safe and effective operation of many components on naval and commercial ships. In order to be operated under local power (for various mission-critical reasons) they need to consume as little energy as possible in order to ensure continued operability. This paper focuses on optimized design of a typical system using high fidelity nonlinear dynamic models for all the subsystems with full consideration of stability constraints. A simulated annealing algorithm is applied to explore optimal design using two sets of design variables. The results indicate that substantial amount of energy can be saved by an intelligent design that helps select parameters carefully, but also uses hydrodynamic loads to augment the closing effort. [DOI: 10.1115/1.4024720]

1 Introduction

Typical automation systems used in the US Navy consist of actuators, sensors, controllers, valves, piping, electrical cabling, and communication wiring. Many types of actuator-valve systems are in use Refs. [1,2].

The main objective of the smart valves is to shut down automatically in case of breakage and to reroute the flow as needed. The future intention is to operate them under local power which means that they need to consume as little energy as possible in order to ensure continued operability. These are typically large valves that consume significant energy with complex nonlinearities, and hence energy optimization is difficult, but could have a high pay-off.

In recent research, we have derived high fidelity mathematical models for the coupled system [3] and analyzed the nonlinear dynamics [4]. Our results have shown that the behavior is complex and surprising with unstable behavior in some parameter ranges; operating in these regimes would (at least) result in unwanted vibration and possibly lead to catastrophic damage. Other results we have reported [5] include quintessentially nonlinear dynamic behavior such as jump phenomena leading to interruption of operation, sudden dynamic loads, transient chaos (shown in Fig. 1), and structural damage. The focus in this paper is on improvements in the design of this complex system in order to achieve optimal configurations.

Contributed by the Design Automation Committee of ASME for publication in the JOURNAL OF MECHANICAL DESIGN. Manuscript received January 5, 2012; final manuscript received May 6, 2013; published online July 2, 2013. Assoc. Editor: Zissimos P. Mourelatos.

Optimization of solenoid actuators has received much attention to overcome rising concerns of energy used. Ju and Woong [6] have focused on the optimal design of solenoid actuators using a nonmagnetic ring. Electromagnetic actuator-current development has been researched by Hameyer and Nienhaus [7], and Sung et al. [8] studied development of a design process for on-off type of solenoid actuators.

This paper starts with a brief résumé of the mathematical model extracted from [3], provided here for completeness. The system parameters are lumped into a nondimensional and meaningful set; then, with the aid of nonlinear dynamic analysis the nominal response of the valve is derived by selecting some reasonable and practical variables ensuring that the system stability requirements are satisfied at all times [9]. Then, the optimal design process is formulated and carried out to guide in the selection of system parameters associated with the electromagnetic actuation, geometry, and mechanical design in order to create an energy efficient system.

2 Mathematical Modeling

The system consists of a solenoid actuator energized by an electric voltage (DC or AC) which moves a plunger. The plunger is connected to a butterfly valve through a rack and pinion arrangement as shown in Fig. 2(*a*). The magnetic flux generates the needed electromagnetic force to move the plunger and subsequently results in the rotation of the butterfly valve by the coupled rack and pinion mechanism. Note that we utilized a return spring for the valve opening; this is a common practice among manufacturers. Also note that the analysis is focused on the closing process, which is the most critical function of the smart valve.

Following the free body diagram (Fig. 2(*b*)), the coupled dynamical equations of the plunger and butterfly valve and the rate of current can be written as follows. A kinematic constraint governs the rack and the pinion mechanism ($x = r\alpha$).

$$\frac{di}{dt} = \frac{(V - Ri)(R_1 + R_2(g_0 - x))}{N^2} - \frac{R_2 i\dot{x}}{(R_1 + R_2(g_0 - x))} \tag{1}$$

$$\begin{aligned}\left(mr^2 + J\right)\ddot{\alpha} + \left(cr^2 + b\right)\dot{\alpha} + kr^2\alpha \\ = \frac{rR_2N^2i^2}{2(R_1 + R_2(g_0 - r\alpha))^2} + \frac{32\rho T_c D_v^3 V_0^2}{3\pi[C_{cc}(1 - \sin(\alpha))]^2} \\ - \frac{\pi}{16}\mu\rho D_s D_v^2 V_0^2 \operatorname{sign}(\dot{\alpha})\left(\frac{2}{C_{cc}(1 - \sin(\alpha))} - 1\right)^2 - C_s D_v^2\end{aligned} \tag{2}$$

where g_0 indicates the maximum stroke of the plunger, N is the number of coils, i is the applied current, V is the supply voltage, R indicates the electrical resistance of coil, x is the displacement of

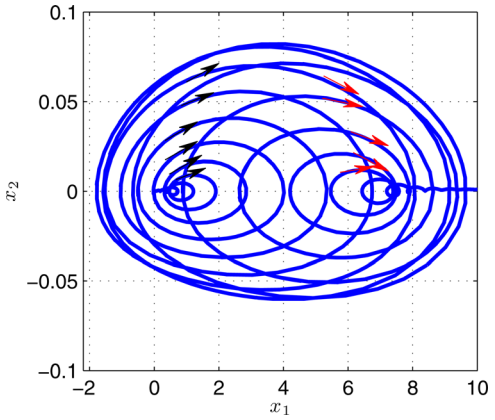

Fig. 1 Transient chaotic motion for some critical values captured from the nonlinear dynamic analysis

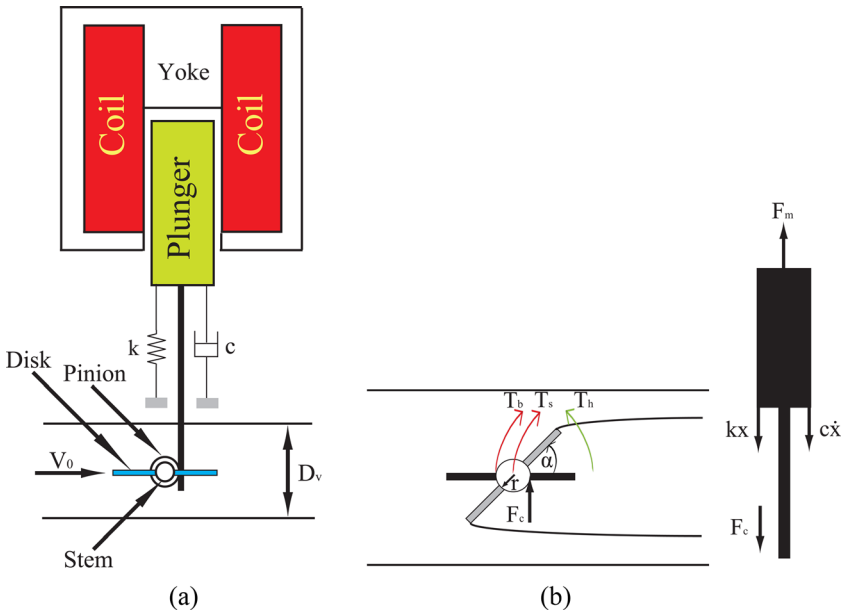

Fig. 2 (*a*) Schematic model of the system; (*b*) free body diagrams of the solenoid actuator and the butterfly valve

solenoid plunger, R_1 and R_2 are the reluctances of the magnetic flux paths, ρ is the fluid density; α is the valve rotation angle; T_c indicates the torque coefficient which can be calculated by a look-up table for various values of α based on computational fluid dynamics calculations; D_v is the pipe diameter; V_0 indicates the inlet velocity of flow; V_J is the jet velocity; C_{cc} is the sum of upper and lower contraction coefficients; D_s is the stem diameter; μ indicates the friction coefficient of the bearing area; C_s is the coefficient of the seating area; and $\Delta P = \frac{1}{2}\rho V_0^2((V_J/V_0)-1)^2$ is the pressure drop across the valve. Note that C_{cc} and T_c are dependent on the valve angle, α. Equations (1) and (2) constitute the third order dynamic model for the system.

3 Nondimensionalization

In order to reduce the number of parameters, and to perform a systematic analysis, the nonlinear dynamic equations need to be nondimensionalized. We define the state vector as $x = [\alpha, \dot{\alpha}, i]^T$, and derive the nondimensionalized state-space equations as follows:

$$\dot{x}_1 = x_2 \tag{3}$$

$$\dot{x}_2 = -x_1 - 2\zeta x_2 + \frac{\vartheta x_3^2}{(\Delta_1 + \Delta_2(\gamma - x_1))^2} + \overbrace{(x_1(\beta_1 e^{\alpha x_1} + \beta_2))}^{T_h} - \text{sign}(x_2)\overbrace{(\kappa_1 x_1^2 e^{\kappa_2 x_1} + \kappa_3 e^{\kappa_4 x_1})}^{T_b} - \frac{C_s D_v^2}{\omega_{n0}^2(J + mr^2)} \tag{4}$$

$$\dot{x}_3 = \frac{(v - x_3)(\Delta_1 + \Delta_2(\gamma - x_1))}{N^2} - \frac{\Delta_2 x_2 x_3}{(\Delta_1 + \Delta_2(\gamma - x_1))} \tag{5}$$

Here

$$\omega_{n0} = \sqrt{\frac{kr^2}{J + mr^2}}; \quad \gamma = \frac{g_0}{r}; \quad \Delta_1 = \frac{\text{RR}_1}{\omega_{n0}}; \quad \Delta_2 = \frac{\text{RR}_2 r}{\omega_{n0}}$$

$$\zeta = \frac{(b + cr^2)}{2\omega_{n0}(J + mr^2)}; \quad \vartheta = \frac{rR_2 N^2 i_0^2 R^2}{2\omega_{n0}^4(J + mr^2)}$$

where T_b is the bearing torque and T_h is the hydrodynamic torque. Note that the sign function is replaced by a differentiable function $(\text{sign}(x_2) \approx \tanh(Kx_2))$. K can be tuned to get a good approximation; we used $K = 1$ in this analysis.

4 Optimal Design

A systematic optimal design procedure is necessary to achieve energy optimization as well as safe and stable operation. Even for the process of obtaining a "nominal" design, it is necessary to ensure that the system is in the stable domain [9].

The problem is one of constrained optimization with possibly several local minima. The design variables need to be selected based on practical considerations and those that one would not have the freedom to select at will because of other pragmatic constraints would need to be excluded. Their lower and upper bounds need to be specified again from practical considerations. The constraints are the state equations and the stability constraints.

We wish to minimize the cumulative energy usage which leads to the following objective function.

$$\min E = \int_0^{t_f} vidt \tag{6}$$

Certain parameters are fixed because of other constraints such as the pipe diameter, applied voltage, etc.; hence much of the design here concerns the actuation subsystem. After choosing some of the variables as predetermined, the design variables for the optimization problem are chosen to be as follows: ϑ is the magnetic force coefficient, Δ_1 indicates the sum of nondimensional reluctances of the magnetic flux paths except the air gap including design parameters such as the path lengths, the cross-sectional areas, and the material permeabilities, Δ_2 is related to the reluctance of the air gap, γ is a geometrical parameter, and N stands for the number of coils. It is helpful to categorize the system optimization as two distinct problems: excluding the number of coil windings (N) as a design variable, and including it.

Hence, the design variables can be put into the following form depending on whether or not we choose to include N as a design variable.

$$\theta_1 = [\vartheta, \Delta_1, \Delta_2, \gamma]^T, \quad \theta_2 = [\vartheta, \Delta_1, \Delta_2, \gamma, N]^T \tag{7}$$

We require that the state equations (Eqs. (3)–(5)) are satisfied at all times during the optimization process. In addition, the design variables are subject to the following lower and upper bounds:

$$\theta_{\min} = [3.8 \times 10^6, 530, 10^4, 1.6, 1500]^T \tag{8}$$

$$\theta_{\max} = [4.8 \times 10^6, 537, 1.1 \times 10^4, 2.6, 1900]^T \tag{9}$$

These bounds were estimated from practical considerations.

We utilize the simulated annealing algorithm for optimization. The method was independently developed by Kirkpatrick et al. [10] and by Cerny [11]. Note that there are alternative tools such as "Multistart Optimization" to achieve the same objective.

The design variables in practice are not of the same order, and caused serious numerical errors in our initial studies. We solved this problem by conditioning them using a normalization scheme as follows:

$$N_n = \frac{N}{10^3}; \quad \vartheta_n = \frac{\vartheta}{10^6}; \quad \Delta_{1n} = \frac{\Delta_1}{10^2}; \quad \Delta_{2n} = \frac{\Delta_2}{10^4}$$

We also used random starts for the optimization process (as required by simulated annealing) as follows:

$$\theta_{\text{nr}} = \theta_{\text{lb}} + (\theta_{\text{ub}} - \theta_{\text{lb}}) \times \text{rand}(0, 1) \tag{10}$$

where rand(0,1) indicates a random number between zero and one. The algorithm was implemented in MATLAB and yielded many interesting results which we discuss in the sequel.

5 Results

Figure 3(*a*) compares optimal and nominal valve phase portraits indicating similar angular velocities and stable responses; hence, the optimal path does not create higher dynamic loads than the nominal case. For both the responses, "uphill" and "downhill" profiles could easily be observed. This is due to an interesting interaction between the hydrodynamic and bearing torques (explained below), which is very useful information for safe design and operation of the system.

We have shown [9] that the bearing torque, as a resisting factor for the valve closing process and also affected directly by the pressure drop across the valve, takes higher values in the domain above 60 deg, whereas the hydrodynamic torque (which aids the closing process), takes considerably lower values in comparison with the bearing torque. This can be seen in Figs. 3(*b*) and 3(*c*). This leads to the "uphill" profile seen in Fig. 3(*a*) indicating an accelerating motion; the hydrodynamic torque may play a more effective role than the bearing torque to help the valve to close for the region under 60 deg. The bearing torque becomes significant when the pressure drop reaches a high value (above 60 deg). Consequently, the "downhill" profile for the decelerating motion comes from the powerful and resisting bearing torque which clearly results in a considerably slower response of the valve for the rest of its motion. It is also important to note the stabilizing role of the bearing torque [9] to stop the valve when it reaches its closing position.

These remarks about the behavior of the torques help us obtain a physical interpretation for the phase portrait shown in Fig. 3(*a*). The optimization process yields higher values of the hydrodynamic and bearing torques for the region discussed than for the nominal response. This seems to indicate that, in addition to a suitable choice of some of the geometric parameters, the optimal design essentially exploits the fluid dynamics to achieve energy minimization.

The energy optimized can be visualized by looking at the system current and energy consumption shown in Figs. 3(*d*) and 4(*a*).

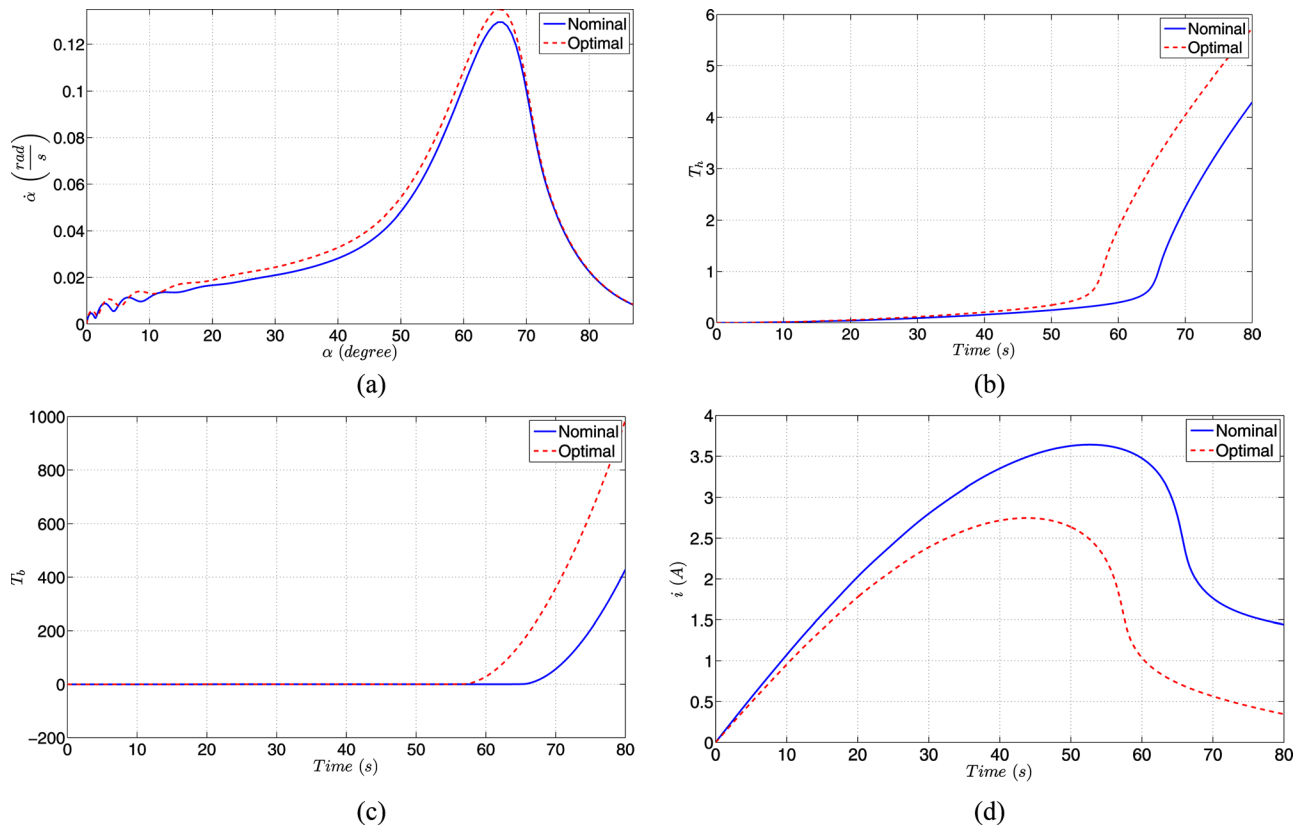

Fig. 3 (*a*) Valve angular velocities versus α for the nominal and optimal responses; (*b*) hydrodynamic torques for the nominal and optimal responses; (*c*) bearing torques for the nominal and optimal responses; and (*d*) the current used for the nominal and optimal responses

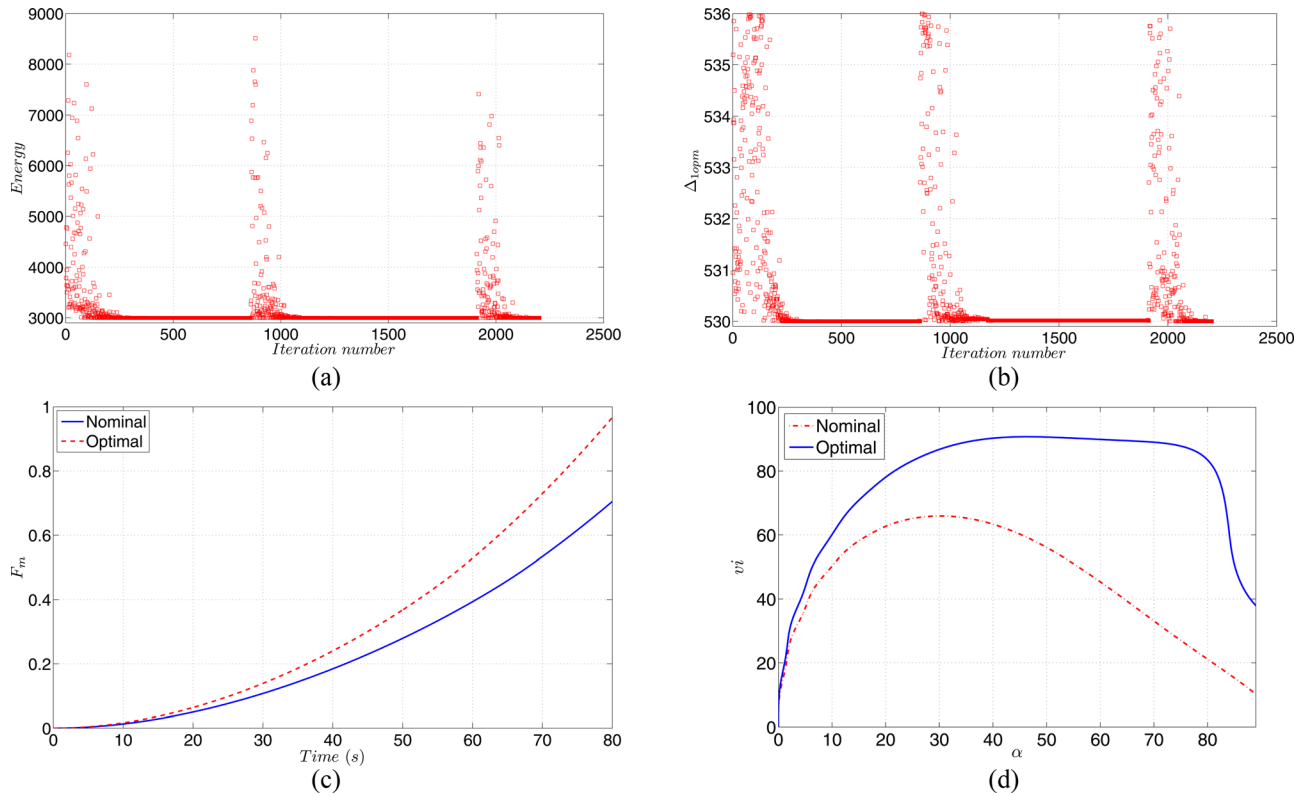

Fig. 4 (*a*) Energy used for the optimal response; (*b*) the optimized Δ_1; (*c*) the applied magnetic forces versus time for the nominal and optimal responses; and (*d*) instantaneous consumption of the system energy versus α for the nominal and optimal responses

It is clear that the current values are lower for the optimal response compared to the nominal response. Also, the energy saved is upward of 41%.

Our understanding of the torques' behavior enables us to analyze the current behavior shown in Fig. 3(*d*). We can observe considerably lower values of the current optimized for the region above 60 deg. Again, this is a result of the fact that the hydrodynamic torque, which helps to close the valve, is higher for the optimized system reducing the need for a high current.

Figure 4(*b*) illustrates the optimization process for Δ_1. As would be expected, much longer calculation time is needed for the algorithm than would be needed for a "one-shot" optimization which would have invariably converged to a local minimum. The process for the simulated annealing algorithm is shown in Fig. 4(*b*) presenting three random samples of the domain for Δ_1 in order to escape from a possible local minimum. The algorithm terminates after 2050 iterations satisfying the tolerances defined for both the cost function and the design variables.

The list of parameters given in Table 1 is interesting in that all the parameters regulate the actuation force and the current terms. ϑ has a higher value, while Δ_1, Δ_2, and γ are lower yielding an increase in the value of the magnetic force. Physically, Δ_1 and Δ_2 are the reluctances of the magnetic paths and clearly their smaller values due to the optimization process would help the magnetic flux flows easily. γ, as the ratio of the nominal air gap and the pinion radius, contributes in increasing the magnetic force; its smaller value can be translated as a smaller air gap (by fixing r); and hence a weaker resistance against the magnetic flux. We logically expect higher values for the magnetic force, which would permit lower values of the current. Consequently, one has a lower value for the system energy usage. This fact is also supported by the magnetic force profiles shown in Fig. 4(*c*) where the higher values of the force are distinguishable for the optimal response.

Table 1 The nominal and optimal parameters

Nominal		Optimal	
Δ_{1n}	536	Δ_{1o}	530
Δ_{2n}	1.1×10^4	Δ_{2o}	10^4
ϑ_n	3.8×10^6	ϑ_o	4.8×10^6
γ_n	1.8	γ_o	1.6
N_n	2000	N_o	1830

Also shown in Fig. 4(*d*) is the instantaneous consumption of the system energy versus the valve rotation angles for both the nominal and optimal responses, which is quite instructive. For the optimal response, the instantaneous energy is lower for higher rotation angles, whereas we might have expected the opposite behavior should we not have had a clear understanding of the role of the torques as explained earlier.

As stated earlier, we also investigated N as an additional design parameter in order to investigate its probable effects on the optimal response of the system. It can easily be shown that the number of coils and the energy used have a mutual interaction in the sense that an increase in the number of coils yields a higher value for the energy used; this hence helps us to determine the upper bound of N. The lower bound needs to be determined based on constraints derived from system stability [9].

A higher degree of optimality was captured for the set containing N as the design variable by yielding a faster response of the second set, θ_2. Note that the arguments made for the first set, θ_1, are also valid for the second set, θ_2. The percentage of energy difference between the two cases is 1.6% and is not so significant as to make a real difference.

6 Conclusions

This paper focused on the optimal design of an important practical problem of actuated smart valves. Nonlinear optimal design

tools were utilized to minimize the system energy used for two sets of design variables. Design for minimum energy is indeed critical to the operation of this system and will contribute significantly toward advances in shipboard autonomy.

It is important to enforce stability constraints as we have shown previously from nonlinear dynamic analysis that the system exhibits instabilities, bifurcations, and chaos.

The principal results of this paper can be summarized as follows.

- Energy can be saved by a significant amount (as much as 41%) by implementing optimal design.
- The optimal design essentially exploits the fluid dynamics to achieve energy minimization.
- Lower values of the current and energy particularly for higher rotation angles are optimal.
- Higher values of the magnetic actuation force, hydrodynamic and bearing torques are observed in the optimal response.
- A slightly better optimal performance would be obtained if the number of windings, N is also a design variable.

We are currently focusing on shaping the valve profile to seek optimality due to the dynamic performance of the system.

Acknowledgment

This work was supported by Office of Naval Research Grant (N00014/2008/1/0435). The authors are grateful to ONR, and Mr. Anthony Seman III in particular, for the financial support that made this research possible. Thanks are also due to Dr. Stephen Mastro and Mr. Frank Ferrese of Naval Surface Warfare Center (Philadelphia) for valuable help and guidance.

References

[1] Hughes, R., Balestrini, S., Kelly, K., Weston, N., and Mavris, D., 2006, "Modeling of an Integrated Reconfigurable Intelligent System (IRIS) for Ship Design," Proceedings of the 2006 ASNE Ship and Ship Systems Technology (S3T) Symposium.

[2] Lequesne, B., Henry, R., and Kamal, M., 1998, "Magnavalve: A New Solenoid Configuration Based on a Spring-Mass Oscillatory System for Engine Valve Actuation," GM Research Report E3-89.

[3] Naseradinmousavi, P., and Nataraj, C., 2011, "Nonlinear Mathematical Modeling of Butterfly Valves Driven by Solenoid Actuators," Appl. Math. Model., **35**(5), pp. 2324–2335.

[4] Naseradinmousavi, P., and Nataraj, C., 2012, "Transient Chaos and Crisis Phenomena in Butterfly Valves Driven by Solenoid Actuators," Commun. Nonlinear Sci. Numer. Simul., **17**(11), pp. 4336–4345.

[5] Kwuimy, C. A. K., and Nataraj, C., 2012, "Modeling and Dynamic Analysis of a Magnetically Actuated Butterfly Valve," Nonlinear Dyn., **70**(1), pp. 435–451.

[6] Baek-Ju, S., and Eun-Woong, L., 2005, "Optimal Design and Speed Increasing Method of Solenoid Actuator Using a Non-Magnetic Ring," International Conference on Power Electronics and Drives Systems, pp. 1140–1145.

[7] Hameyer, K., and Nienhaus, M., 2002, "Electromagnetic Actuator-Current Developments and Examples," 8th International Conference on New Actuators, pp. 170–175.

[8] Sung, B. J., Lee, E. W., and Kim, H. E., 2002, "Development of Design Program for on and off Type Solenoid Actuator," Proceedings of the KIEE Summer Annual Conference, Vol. B, pp. 929–931.

[9] Naseradinmousavi, P., and Nataraj, C., 2011, "A Chaotic Blue Sky Catastrophe of Butterfly Valves Driven by Solenoid Actuators," Proceedings of the ASME 2011 International Mechanical Engineering Congress & Exposition, No. IMECE2011/62608.

[10] Kirkpatrick, S., Gelatt, C. D., and Vecchi, M. P., 1983, "Optimization by Simulated Annealing," Science, **220**(4598), pp. 671–680.

[11] Cerny, V., 1985, "Thermodynamical Approach to the Traveling Salesman Problem: An Efficient Simulation Algorithm," J. Optim. Theory Appl., **45**(1), pp. 41–55.